

Deep level transient spectroscopy and minority carrier lifetime study on Ga-doped continuous Czochralski silicon

Yohan Yoon,^{1,a)} Yixin Yan,¹ Nels P. Ostrom,² Jinwoo Kim,^{3,a)} and George Rozgonyi¹

¹Department of Materials Science and Engineering, North Carolina State University, Raleigh, North Carolina 27695, USA

²GT Advanced Technologies, Hazelwood, Missouri 63042, USA

³Department of Physics, North Carolina State University, Raleigh, North Carolina 27695, USA

(Received 18 September 2012; accepted 23 October 2012; published online 27 November 2012)

Continuous-Czochralski (c-Cz) crystal growth has been suggested as a viable technique for the fabrication of photovoltaic Si wafers due to its low resistivity variation of any dopant, independent of segregation, compared to conventional Cz. In order to eliminate light induced degradation due to boron-oxygen traps in conventional p-type silicon wafers, gallium doped wafers have been grown by c-Cz method and investigated using four point probe, deep level transient spectroscopy (DLTS), and microwave-photoconductance decay. Iron-gallium related electrically active defects were identified using DLTS as the main lifetime killers responsible for reduced non-uniform lifetimes in radial and axial positions of the c-Cz silicon ingot. A direct correlation between minority carrier lifetime and the concentration of electrically active Fe-Ga pairs was established. © 2012 American Institute of Physics. [<http://dx.doi.org/10.1063/1.4766337>]

The significant minority carrier lifetime degradation observed in boron doped p-type Czochralski (Cz) Si is mainly caused by two issues: iron-boron (FeB) pair traps and boron-oxygen (B-O) driven light induced degradation (LID). To suppress LID, the replacement of B by Ga as a p-type dopant has been proposed.^{1–6} In spite of the effective elimination of B-O related defects, Ga-related pairing with iron, oxygen, and carbon can also reduce lifetime.^{3,6} Moreover, the resistivity of Ga doped Si ingots, grown using conventional Cz, varies along the growth axis due to the low segregation coefficient (0.08).⁷ Although the varying resistivity of Ga-doped Si can be mitigated with changes in cell processing for fabricating high efficiency solar cells,⁴ the cost of these changes is not economically viable, making it expensive to utilize traditionally grown crystal.⁸ As an alternative, the Continuous-Czochralski (c-Cz) method in which the crucible is refilled by adding polycrystalline silicon chips has been developed for uniform resistivity. Even though theoretical models and experimental growth of Ga-doped C-Cz Si and Ga segregation for Cz Si co-doped with B^{4,9,10} have been studied, very limited data are available on the distributions of dopants and defects and their correlations with minority carrier lifetime in axial and radial directions. This paper provides detailed information on the electrical properties of Ga doped c-Cz Si samples, wherein the resistivities and minority carrier lifetimes in different positions of a Si ingot were correlated to deep energy levels using deep level transient spectroscopy (DLTS). Especially, Ga related defects as lifetime killers have been identified and quantified and their dissociation by low temperature annealing determined.

Six-inch diameter, Ga-doped (concentration $\sim 1 \times 10^{15} \text{ cm}^{-3}$, p-type), 3-mm-thick c-Cz Si samples from various positions along the ingot height (38, 730, and 888 mm from the seed of the ingot) were selected for lifetime and deep

energy level measurements. Samples from the center, middle, and edge of each sample were selected for evaluation of the radial variation of lifetime and deep energy levels. Each sample was mechanically polished and RCA (a recipe developed by the RCA (Radio Corporation of America)) cleaned. Resistivities were measured using four point probe (4PP). The as-grown data were collected directly from silicon samples that were cut from the ingot. The post-anneal samples were measured after a heat treatment at 750 °C for 30 min and quenched in air. Minority carrier lifetimes were measured using the microwave-photoconductance decay (MW-PCD) technique with the samples immersed in an iodine-ethanol solution during the lifetime measurements for surface passivation. A Bio-Rad DL8000 DLTS system was used to determine the concentration and trap energy of electrically active defects. Aluminum Schottky diodes under a 3 V reverse bias were pulsed for 50 μs at 0 V to obtain DLTS data from 40 K to 298 K. Finally, dissociation of electrically active defects was studied following annealing for 2 min at 250 °C and 300 °C in a vertical tube furnace under argon (Ar) ambient, followed by slow cooling in air.

Figure 1(a) shows resistivities of as-grown and post-anneal samples in radial and axial positions of the Ga-doped c-Cz Si. The as-grown data are the resistivity due to the Ga dopant and the thermal donors formed during the crystal growth process. The thermal donors, which are due to oxygen, compensate the Ga atoms but are removed from the crystal during the annealing. The post-anneal resistivity is due to the intentional Ga doping only. Figure 1(b) more clearly shows the resistivity control of the c-Cz process by comparing the as-grown and post-anneal data from the center of the ingot. The variation of resistivity from seed to tail was around 0.2 $\Omega \text{ cm}$ (2.1–1.9 $\Omega \text{ cm}$) which is less than 10%. This value is smaller than that of conventional B-doped Cz Si and is much smaller than that of conventional Ga-doped Cz Si.¹¹ Although the resistivity variation of the postannealed samples is low, Ga concentration variations still exist. Theoretically, in

^{a)} Authors to whom correspondence should be addressed. Electronic addresses: yyoan3@ncsu.edu and jinwookim1@gmail.com.

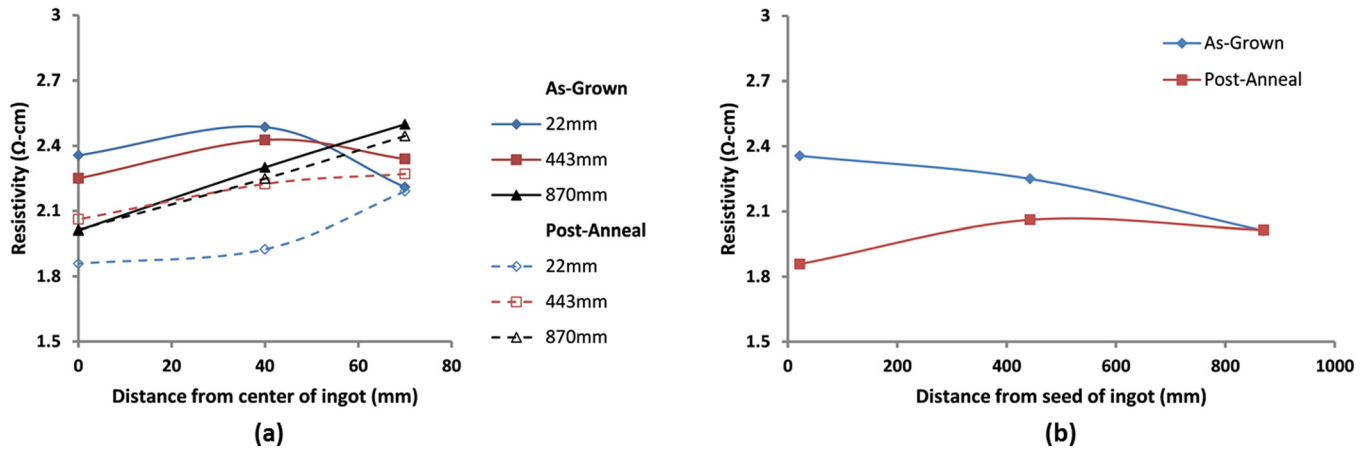


FIG. 1. Resistivities of (a) as-grown and post-anneal samples in radial and axial positions and (b) as-grown and post-anneal samples in the center of ingot.

continuous Cz process, almost constant resistivities can be achieved by process optimization, e.g., the replenishment of polysilicon, the pulling conditions, the experimental apparatus, etc.^{12,13} According to the theoretical model, the concentrations of impurities at the interface of the melting and solidified Si can be expressed as a function of the dimensionless dilution rate (β) and the segregation coefficient of the impurity (k). Uniform radial and axial distributions of the dopants can be achieved by adjusting β according to k .¹² As for the growth of the samples for this study, the axial profile of the resistivity is a good example of what can be produced

in a cost-effective production environment. The growth process was changed to introduce a larger radial gradient for this work.

Figure 2 shows DLTS spectra for samples at various radial and axial positions of the c-Cz Si ingot. Four hole traps; labeled as H1, H2, H3, and H4, have energy levels of 0.13, 0.23, 0.36, and 0.44, respectively. Table I lists the chemical identifications, trap densities, and capture cross sections of each of the four hole traps.

The hole traps H1 at 80 K and H2 at 120 K are attributed to iron-gallium pairs ($\text{Fe}_i\text{-Ga}_s$) with different charge states. The hole trap H1 corresponds to the metastable $\langle 111 \rangle$ configuration and H2 corresponds to the stable $\langle 100 \rangle$ configuration, and their transformations are completely reversible.^{14–17} H1 and H2 were either observed together or negligible on each sample. There are three possible origins of the hole trap H3: (1) interstitial iron-self-interstitial-silicon complex (Fe_iSi_i),¹⁸ (2) interstitial iron-vacancy complex (Fe_iV),^{20,21} and (3) interstitial-carbon-interstitial-oxygen complex (Ci-O_i).^{18–20} Native point defects such as silicon self-interstitials (Si_i) and vacancies (V) usually exist in Cz Si, although neither of their concentrations are high.^{21,22} Ci-O_i was less likely to dominate in our case since high concentration of interstitial carbon (C_i) is required to form Ci-O_i and the dominant light impurity is substitutional carbon (C_s) rather than interstitial carbon (C_i) in Cz Si. The identification of H3 was investigated further by dissociation during thermal annealing. The hole trap H4 is attributed to interstitial iron (Fe_i), as a common metallic impurity in Cz Si.¹⁷ The origin of the trap H4 was also confirmed by its annealing behaviors.

As shown in Fig. 2, the compositions of the peaks at different axial position (38, 730, and 880 mm) in the ingot are consistent; however, their concentrations change with radial positions (center, middle, and edge). While center samples exhibit all four peaks regardless of their axial positions,

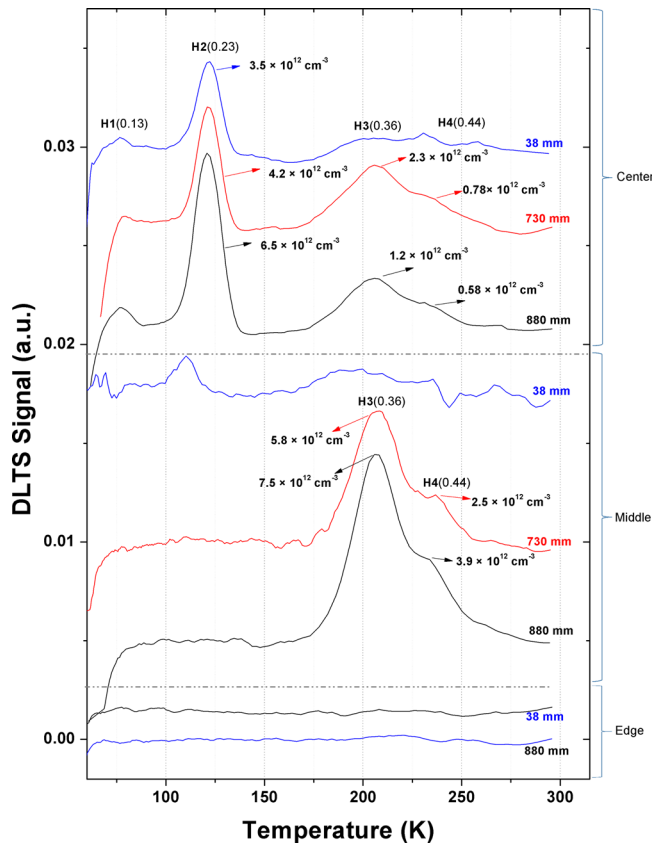


FIG. 2. DLTS spectra (scale shift) of samples near the center, the middle, and the edge of samples at heights of 38 mm, 730 mm, and 880 mm, respectively. The spectra were acquired using a reverse bias of 3 V, a pulse voltage of 0 V, a pulse width of 5×10^{-5} s, and a period width of 50 ms.

TABLE I. Activation energies (E_a) and carrier capture cross-sections (σ) of four peaks in FIG. 1.

Identification	H1 ($\text{Fe}_i^+\text{-Ga}_s$)	H2 ($\text{Fe}_i^0\text{-Ga}_s$)	H3 ($\text{Fe}_i\text{V}/\text{Fe}_i\text{Si}_i$)	H4 (Fe_i)
E_a (eV)	0.13	0.23	0.36	0.44
σ (cm ²)	2.5×10^{-14}	5.5×10^{-15}	3.3×10^{-16}	3.8×10^{-16}

samples in the middle only show spectral peaks H3 and H4, while edge samples have no signal detected above the DLTS detection limit of $1 \times 10^{11} \text{ cm}^{-3}$. The non-uniform axial distribution of the electrically active defects is attributed to the low segregation coefficient of Fe ($k_0 = (5-7) \times 10^{-6}$)^{23,24} and the effective segregation coefficient which is reported to be smaller than 0.05.²⁵ Therefore, iron segregates in both center and bottom areas of the Si ingot. The increase in signal intensity of H2 clearly shows the increase of Fe concentration from seed to tail. Also, Ga segregates at the center areas due to its relatively low segregation coefficient.²⁶ Also both Fe and Ga evaporate from the melt and their concentrations are low at the edge and middle areas of the crystal. Therefore, Fe-Ga pairs (H1 and H2) are present in the center of the samples regardless of the axial positions, but absent in the middle and edge areas, see Fig. 2. The surface of the ingot is a sink for silicon interstitials, so H3 and H4 peaks are absent in the edge areas. Similar to Fe-B pairs, the equilibrium of Fe-Ga pair reaction depends on the temperature and the Ga concentration. The study on Fe-B pair reactions showed that the interstitial fraction ($[\text{Fe}_i]/[\text{Fe}] = [\text{Fe}_i]/([\text{Fe}_i] + [\text{FeB}])$) increased with temperature but decreased with B concentration.²⁷ Similar behaviors are applicable to Ga-doped samples. Therefore, the total amount of electrically active Fe is the sum of the interstitial Fe concentration and Fe-Ga pairs. The dissociation or association of the Fe-Ga pair will be discussed in the annealing behavior study below.

Minority carrier lifetimes were measured for three samples in the center areas of various axial positions (38, 790, and 880 mm) from the seed. Fig. 3 shows the direct correlation between the lifetimes and the concentrations of Fe-Ga defects. The sample at the height of 38 mm has the highest lifetime and the lowest concentration of Fe-Ga pairs, and the sample at 880 mm has the lowest lifetime and the highest concentration of Fe-Ga pairs. This indicates that the concentration of Fe-Ga pairs is more detrimental to minority carrier lifetime than that of Fe_i . The main reason is the comparatively large electron-capture cross section σ_n ($2.5 \times 10^{-14} \text{ cm}^2$) of Fe-Ga pairs.^{6,28}

In order to verify the identity of peak H3 ($\text{Fe}_i\text{V}/\text{Fe}_i\text{Si}_i$) and the thermal stability of Fe-Ga pairs, the middle wafer

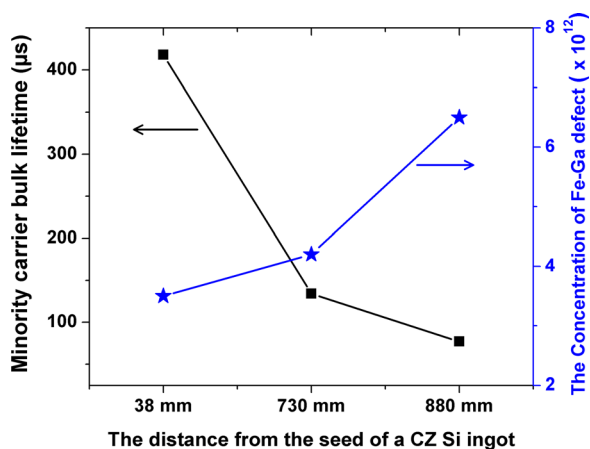


FIG. 3. The concentration of Fe-Ga and minority carrier bulk lifetime of the samples of the center of the wafers along a CZ-Si ingot height. The distance is from the seed of the ingot.

880 mm sample was annealed at 250 and 300 °C. The DLTS spectra for the control and the annealed samples are shown in Fig. 4. The intensity of H3 ($\text{Fe}_i\text{V}/\text{Fe}_i\text{Si}_i$) decreases significantly while those of H1, H2, and H4 increase during annealing due to the dissociation of $\text{Fe}_i\text{V}/\text{Fe}_i\text{Si}_i$ pairs. It is clearly proved that the hole trap H3 is associated with Fe_iSi_i pair due to its dissociation temperature ($\sim 250^\circ\text{C}$).¹⁸ The interaction between Fe and V is more energetic than that between Fe and Si_i ; thus, the dissociation temperature of the Fe_iV pair is comparatively higher ($\sim 400^\circ\text{C}$).^{19,20} Furthermore, the relatively high dissociation temperature of the $\text{C}_i\text{-O}_i$ pair ($\sim 400^\circ\text{C}$)³ excludes the possible identification of the hole trap H3 as $\text{C}_i\text{-O}_i$ trap level.

The dissociation of the hole trap H3 induces the appearance of the hole traps Fe-Ga pairs (H1 and H2) and Fe_i pairs (H4). However, the H3 and H4 pairs increase at higher annealing temperature (300 °C) due to the dissociation of Fe-Ga pairs. As mentioned in the discussion on defect composition, the fraction of Fe_i could be expressed as a function of the temperature and the dopant concentration. Thus, when the annealing temperature increases from 250 to 300 °C, $\text{Fe}_i\text{V}/\text{Fe}_i\text{Si}_i$ pairs are further dissociated, and even Fe-Ga bonds also are broken, contributing to a larger fraction of Fe_i .²⁷ Moreover, all the changes in the intensities of the peaks confirmed the identification of H4 as Fe_i .

In conclusion, resistivity variation and lifetime limiting factors were investigated in c-Cz grown Ga-doped Si. The resistivity variation of c-CZ wafers showed a relatively good uniformity of dopant distribution compared to conventional CZ wafers. The radial and axial variation of electrically active defects were observed in DLTS spectra and correlated

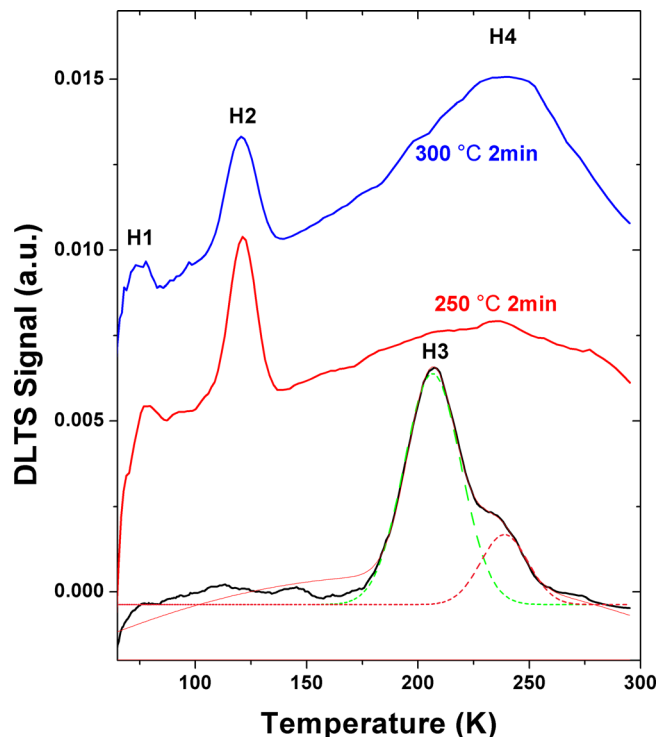


FIG. 4. DLTS spectra of annealed samples from the middle of the CZ-Si ingot 880 mm from the seed. The samples were annealed at 250 and 300 °C for 2 min. The spectra were acquired using a reverse bias of 3 V, pulse voltage of 0 V, pulse width of $5 \times 10^{-5} \text{ s}$, and period width of 50 ms.

to lifetime and resistivity variations. DLTS measurements demonstrated that iron-related pairs are responsible for the variations. Specifically, Fe-Ga pairs were found to be serious recombination sites, which are more detrimental to lifetime than Fe_i. A c-Cz method was found to have potential for fabricating uniformly Ga-doped Si for high performance solar cells, but the issue of iron contamination still needs to be addressed.

- ¹S. W. Glunz, S. Rein, J. Y. Lee, and W. Warta, *J. Appl. Phys.* **90**, 2397 (2001).
- ²M. Arivanandhan, R. Gotoh, K. Fujiwara, and S. Uda, *Appl. Phys. Lett.* **94**, 072102 (2009).
- ³A. Khan, M. Yamaguchi, Y. Ohshita, N. Dharmarasu, K. Araki, T. Abe, H. Itoh, T. Ohshima, M. Imaizumi, and S. Matsuda, *J. Appl. Phys.* **90**, 1170 (2001).
- ⁴J. Schmidt, *Solid State Phenom.* **95–96**, 187 (2004).
- ⁵S. W. Glunz, S. Rein, J. Knobloch, W. Wettling, and T. Abe, *Prog. Photovoltaics* **7**, 463 (1999).
- ⁶J. Schmidt and D. Macdonald, *J. Appl. Phys.* **97**, 113712 (2005).
- ⁷F. A. Trumbore, *Bell Syst. Tech. J.* **39**, 212 (1960).
- ⁸A. Anselmo, V. Prasad, J. Koziol, and K. P. Gupta, *J. Cryst. Growth* **131**, 247 (1993).
- ⁹J. H. Wang and J. I. Im, *Jpn. J. Appl. Phys., Part 1* **43**, 4079 (2004).
- ¹⁰X. Huang, M. Arivanandhan, R. Gotoh, T. Hoshikawa, and S. Uda, *J. Cryst. Growth* **310**, 3335 (2008).
- ¹¹V. Meemongkolkiat, K. Nakayashiki, A. Rohatgi, G. Crabtree, J. Nickerson, and T. L. Jester, *Prog. Photovoltaics* **14**, 125 (2006).
- ¹²J. H. Wang, D. H. Kim, and H. D. Yoo, *J. Cryst. Growth* **198–199**, 120 (1999).
- ¹³S. Rein and S. W. Glunz, *J. Appl. Phys.* **98**, 113711 (2005).
- ¹⁴A. Chantre and L. C. Kimerling, “Defects in semiconductors,” *Mater. Sci. Forum* **10–12**, 387 (1986).
- ¹⁵S. Zhao, L. V. C. Assali, J. F. Justo, G. H. Gilmer, and L. C. Kimerling, *J. Appl. Phys.* **90**, 2744 (2001).
- ¹⁶A. Chantre and D. Bois, *Phys. Rev. B* **31**, 7979 (1985).
- ¹⁷A. Istratov, H. Hieslmair, and E. R. Weber, *Appl. Phys. A: Mater. Sci. Process.* **69**, 13 (1999).
- ¹⁸S. Estreicher, M. Sanati, and N. Gonzalez Szwacki, *Phys. Rev. B* **77**, 125214 (2008).
- ¹⁹T. Mchedlidze and M. Suezawa, *Jpn. J. Appl. Phys., Part 1* **41**, 7288 (2002).
- ²⁰H. P. Gunnlaugsson, G. Weyer, N. E. Christensen, M. Dietrich, M. Fanciulli, K. Bharuth-Ram, R. Sielemann, A. Svane, and the ISOLDE Collaboration, *Physica B* **340–342**, 532 (2003).
- ²¹J. Schmidt and A. Cuevas, *J. Appl. Phys.* **86**, 3175 (1999).
- ²²E. R. Weber, *Appl. Phys. A* **30**, 1 (1983).
- ²³J. R. Davis, A. Rohatgi, R. H. Hopkins, P. D. Blais, P. Raichoudhury, J. R. McCormick, and H. C. Mollenkopf, *IEEE Trans. Electron Devices* **27**, 677 (1980).
- ²⁴H. Lemke, in *Semiconductor Silicon/1994*, edited by H. R. Huff, W. Bergholz, and K. Sumino (Electrochemical Society, Pennington, NJ, 1994), p. 695.
- ²⁵D. Macdonald, A. Cuevas, A. Kinomura, Y. Nakano, and L. J. Geerligs, *J. Appl. Phys.* **97**, 033523 (2005).
- ²⁶T. Hoshikawa, X. Huang, S. Uda, and T. Taishi, *J. Cryst. Growth* **290**, 338 (2006).
- ²⁷G. Zoth and W. Bergholz, *J. Appl. Phys.* **67**, 6764 (1990).
- ²⁸K. Wünnel and P. Wagner, *Appl. Phys. A: Mater. Sci. Process.* **27**, 207 (1982).